




# Interferometric geometric phases of $\mathcal{PT}$ -symmetric quantum mechanics

Xin Wang, Zheng Zhou, Jia-Chen Tang, and Xu-Yang Hou <sup>\*</sup>  
*School of Physics, Southeast University, Jiulonghu Campus, Nanjing 211189, China*

Hao Guo <sup>†</sup>  
*School of Physics, Southeast University, Jiulonghu Campus, Nanjing 211189, China  
 and Hefei National Laboratory, University of Science and Technology of China, Hefei 230088, China*

Chih-Chun Chien   
*Department of Physics, University of California, Merced, California 95343, USA*

 (Received 19 January 2024; revised 6 May 2024; accepted 20 May 2024; published 10 June 2024)

We present a generalization of the geometric phase to pure and thermal states in  $\mathcal{PT}$ -symmetric quantum mechanics (PTQM) based on the approach of the interferometric geometric phase (IGP). The formalism first introduces the parallel-transport conditions of quantum states and reveals two geometric phases,  $\theta^1$  and  $\theta^2$ , for pure states in PTQM according to the states under parallel-transport. Due to the non-Hermitian Hamiltonian in PTQM,  $\theta^1$  is complex and  $\theta^2$  is its real part. The imaginary part of  $\theta^1$  plays an important role when we generalize the IGP to thermal states in PTQM. The generalized IGP modifies the thermal distribution of a thermal state, thereby introducing effective temperatures. At certain critical points, the generalized IGP may exhibit discrete jumps at finite temperatures, signaling a geometric phase transition. We illustrate this phenomenon in PTQM through two examples and compare their differences.

DOI: [10.1103/PhysRevB.109.245411](https://doi.org/10.1103/PhysRevB.109.245411)

## I. INTRODUCTION

The introduction of non-Hermitian quantum mechanics (NHQM) [1–3] has uncovered many fascinating phenomena, including Anderson localization [4], gapless quantum phase transitions [5], unconventional behavior of quantum emitters [6,7], tachyonic dynamics [8,9], and distinctive topological properties [10–12]. A major branch of NHQM includes systems with non-Hermitian Hamiltonians obeying parity-time reversal ( $\mathcal{PT}$ ) symmetry, which can possess real-valued eigenvalues, making them a relevant extension of conventional quantum mechanics. Therefore,  $\mathcal{PT}$ -symmetric quantum mechanics (PTQM) has attracted considerable research attention in many aspects [13–19] and has been experimentally realized across different fields, including acoustics, optics, electronics, and quantum systems [20,21]. It has also catalyzed extensive investigations into physical and topological characteristics of non-Hermitian systems [22–30].

Geometric phases in quantum systems, including the Berry phase [31] and the Aharonov-Anandan phase [32], have advanced our understanding of the geometric structures behind interesting physical systems and shown significant influence across various fields. For instance, the Berry phase is fundamental in the study of topological matter since it connects geometric objects from the underlying mathematical structure to measurable physical quantities [33–44]. Recently, the

notion of the geometric phase has been generalized to non-Hermitian quantum systems [45], which is further applied to the construction of the quantum geometric tensor for non-Hermitian systems [46]. On the other hand, the geometric phase has also been generalized to mixed quantum states via different approaches [47–55]. In this work, we will generalize the one proposed by Sjöqvist *et al.* [47] based on an extension of the optical process in the Mach-Zehnder interferometer, which is referred to as the interferometric geometric phase (IGP). Numerous studies [56–61] have been dedicated to this field, and the IGP has been observed by various techniques, including nuclear magnetic resonance [62,63], polarized neutrons [64], and the Mach-Zehnder interferometer [65]. A different approach was introduced by Uhlmann [66–68] soon after the discovery of the Berry phase, and the phase is usually called the Uhlmann phase. This approach incorporates a full mathematical structure based on fiber bundles and has gained attention due to its relevance to condensed matter and quantum information [69–76].

We aim to generalize the concept of IGP to thermal states in PTQM. In the beginning, we establish a formalism for a pure-state geometric phase in  $\mathcal{PT}$ -symmetric systems by using the conventional derivation and then introducing the parallel-transport conditions of quantum states. In contrast to conventional QM, a PTQM system is shown to allow two distinct geometric phases, called  $\theta^1$  and  $\theta^2$ , which are differentiated by the states undergoing parallel-transport. On the one hand,  $\theta^2$  exactly coincides with the known result in Ref. [45] and is the real part of  $\theta^1$ . On the other hand,  $\theta^1$  is a complex-valued phase with its imaginary part

<sup>\*</sup>xuyanghouwow@seu.edu.cn

<sup>†</sup>guohao.ph@seu.edu.cn

adjusting the amplitude of the wave function due to the lack of Hermiticity. Since  $\theta^1$  will be shown to be associated with the non-Hermitian Hamiltonian, the generalization to thermal states in PTQM will be based on it.

Following the construction of the IGP of thermal states in conventional QM and the derivation of the geometric phase  $\theta^1$ , we develop a framework of the IGP of thermal states in PTQM. In general, the IGP is the argument of the thermal-weighted sum of the geometric phase factor for each individual energy level. The imaginary part of the generalized IGP will be shown to alter the relative thermal weights, which introduces effective temperatures to the thermal states. Consequently, there may be quantized jumps of the IGP at certain temperatures and system parameters. This phenomenon signifies a geometric phase transition at finite temperature in PTQM. To illustrate our findings and visualize the results, we study a two-level system and a band model, both possessing  $\mathcal{PT}$  symmetry, and we present their generalized IGPs. The geometric phase transitions of the two models are located and analyzed.

The rest of the paper is organized as follows. Section II briefly reviews the basics of PTQM and its statistical physics. We also review the geometric phases of pure and mixed quantum states in Hermitian systems via parallel-transport. In Sec. III, we generalize the formalism of the geometric phase to PTQM, first by deriving two different expressions due to their associated evolution equations or parallel-transport conditions. We then generalize the results to thermal states in PTQM and derive the generalized IGP. Section IV presents the IGPs of two  $\mathcal{PT}$ -symmetric systems and their geometric phase transitions. Section V concludes our work. Some details and derivations are summarized in the Appendixes.

## II. THEORETICAL BACKGROUND

### A. $\mathcal{PT}$ -symmetric quantum and statistical mechanics

Before presenting our findings, we first give a brief outline of PTQM and lay the foundation for its geometric description. We will set  $c = \hbar = k_B = 1$  throughout the paper. We consider a parameter-dependent finite-dimensional non-Hermitian quantum system described by a  $\mathcal{PT}$ -symmetric Hamiltonian  $H(\mathbf{R})$ . Here  $\mathbf{R} = (R_1, R_2, \dots, R_k)^T$  is a collection of external parameters forming a parameter manifold  $M$ . The system may evolve along a curve  $\mathbf{R}(t)$  in  $M$ . The  $\mathcal{PT}$ -symmetry is manifested by the condition

$$W(\mathbf{R})H(\mathbf{R}) = H^\dagger(\mathbf{R})W(\mathbf{R}), \quad (1)$$

where  $W(\mathbf{R})$  is Hermitian, and its role will become clear later. A Hamiltonian satisfying Eq. (1) is called a pseudo-Hermitian Hamiltonian [77]. Assuming  $H$  describes an  $N$ -level quantum system, the eigenequations of  $H(\mathbf{R})$  and  $H^\dagger(\mathbf{R})$  are given, respectively, by

$$H(\mathbf{R})|\Psi_n(\mathbf{R})\rangle = E_n(\mathbf{R})|\Psi_n(\mathbf{R})\rangle, \quad (2)$$

$$H^\dagger(\mathbf{R})|\Phi_n(\mathbf{R})\rangle = E_n(\mathbf{R})|\Phi_n(\mathbf{R})\rangle \quad (3)$$

for  $n = 1, 2, \dots, N$ . No energy degeneracy is considered here for simplicity. Equation (1) implies  $|\Phi_n(\mathbf{R})\rangle = W(\mathbf{R})|\Psi_n(\mathbf{R})\rangle$ . Here  $W$  bears the role of a metric to ensure the orthonormal relation  $\langle \Psi_m(\mathbf{R})|W(\mathbf{R})|\Psi_n(\mathbf{R})\rangle = \delta_{mn}$ ,

or equivalently,  $\langle \Phi_m(\mathbf{R})|\Psi_n(\mathbf{R})\rangle = \delta_{mn}$ . Thus, the inner product between the ordinary bra and ket states is defined as  $\langle \cdot|W|\cdot\rangle$ . The associated completeness of  $\{|\Psi_n(\mathbf{R})\rangle\}$  is given by  $\sum_n |\Psi_n(\mathbf{R})\rangle\langle \Phi_n(\mathbf{R})| = 1$ .

Following Eq. (1),  $H$  is similar to a Hermitian Hamiltonian  $H_0$  via  $H = SH_0S^{-1}$ , where  $W = (S^{-1})^\dagger S^{-1}$  [78]. The operator  $S$  is not unitary. Hereafter, we sometimes suppress the argument  $\mathbf{R}$  if no confusion may arise. In some situations,  $S$  may also be Hermitian and then  $W = (S^{-1})^2$ . Diagonalizing  $H_0$  as  $H_0|\Psi_n^0\rangle = E_n|\Psi_n^0\rangle$ , one gets

$$|\Psi_n\rangle = S|\Psi_n^0\rangle, \quad |\Phi_n\rangle = (S^{-1})^\dagger|\Psi_n^0\rangle. \quad (4)$$

For a generic time-dependent state  $|\Psi(t)\rangle$  in PTQM, its equation of motion is described by the Schrödinger-like equation [45]:

$$i\frac{d}{dt}|\Psi(t)\rangle = \left(H - \frac{i}{2}W^{-1}\dot{W}\right)|\Psi(t)\rangle. \quad (5)$$

If  $S$  is a proper mapping satisfying  $\dot{S}^{-1}S = (\dot{S}^{-1})^\dagger$ , this equation further reduces to

$$i\frac{d}{dt}|\Psi(t)\rangle = \tilde{H}|\Psi(t)\rangle. \quad (6)$$

Here  $\tilde{H} = H - iS_{\text{proper}}\dot{S}_{\text{proper}}^{-1}$ , with  $S_{\text{proper}}$  being a proper mapping. The second term of  $\tilde{H}$  is anti-pseudo-Hermitian under the  $\mathcal{PT}$  transformation, rendering  $\tilde{H}$  not Hermitian in general. For a PTQM system, a proper  $S$  always exists [45]. However, the analytic expression of  $S_{\text{proper}}$  may not be easily available. Comparing Eqs. (6) and (2), it is important to emphasize that for a  $\mathcal{PT}$ -symmetric quantum system, the stationary and dynamic Schrödinger equations are governed, respectively, by  $H$  and  $\tilde{H}$ . This distinction leads to nontrivial contributions to both the dynamic and geometric phases in PTQM, which will be elucidated in the subsequent discussions. According to Eq. (4),  $|\Psi^0\rangle = S^{-1}|\Psi\rangle$ , and its dynamic evolution can be deduced from Eq. (5). If  $S$  is a proper mapping, it can be shown that  $|\Psi^0(t)\rangle$  obeys the conventional Schrödinger equation

$$i\frac{d}{dt}|\Psi^0(t)\rangle = H_0|\Psi^0(t)\rangle. \quad (7)$$

Otherwise, the dynamic equation of  $|\Psi^0(t)\rangle$  would be very complicated. Further details can be found in Appendix A. In this case, both the stationary and dynamic equations of  $|\Psi^0(t)\rangle$  are governed by the Hermitian  $H_0$ , unlike those of  $|\Psi(t)\rangle$ . Hence, the proper  $S$  acts like a ‘‘gauge’’ mapping between a PTQM system and its corresponding Hermitian counterpart.

So far the discussion concerns pure quantum states only. Recently, there have been studies on non-Hermitian quantum models at finite temperatures [79,80]. To broaden the scope of non-Hermitian physics to mixed quantum states, we note that the density matrix of a mixed state from the generalization may also be non-Hermitian as well. As a first attempt, we focus on states in thermal equilibrium depicted by  $\rho = \frac{e^{-\beta H}}{Z}$ . Here  $\beta = \frac{1}{T}$  is the inverse temperature and  $Z = \sum_n e^{-\beta E_n}$  is the partition function. In the generalized case,  $\rho^\dagger \neq \rho$  due to  $H^\dagger \neq H$ . By expressing  $H = \sum_n E_n|\Psi_n\rangle\langle \Phi_n|$ , the density

matrix is given by

$$\rho = \sum_n \frac{e^{-\beta E_n}}{Z} |\Psi_n\rangle\langle\Psi_n|, \quad (8)$$

whose trace follows the normalization  $\text{Tr}\rho = \sum_n \langle\Psi_n|\rho|\Psi_n\rangle = 1$ . Applying Eq. (4), we get a relation  $\rho = S\rho_0 S^{-1}$  connecting  $\rho$  and  $\rho_0 = \frac{e^{-\beta H_0}}{\text{Tr}e^{-\beta H_0}}$ .

## B. Geometric phase of Hermitian systems

### 1. Pure states

The geometric phase, especially the Berry phase [31], reflects the underlying geometry of quantum physics. For Hermitian systems, its formulation can be derived through the concept of the parallel condition among quantum states. Two states,  $|\psi_1\rangle$  and  $|\psi_2\rangle$ , are considered parallel with each other if  $\langle\psi_1|\psi_2\rangle = \langle\psi_2|\psi_1\rangle > 0$  [81]. The overlap is also referred to as the fidelity [81]. The parallel condition complements the concept of orthogonality of quantum states and builds a binary relation between quantum states. However, it is not an equivalence relation since it lacks transitivity. This means even when a state  $|\Psi(t)\rangle \equiv |\Psi(\mathbf{R}(t))\rangle$  evolves along a path  $\mathbf{R}(t)$  and preserves the condition of instantaneous parallel-transport, or being “in-phase,” denoted as

$$\langle\Psi(t)|\Psi(t+dt)\rangle > 0, \quad (9)$$

it is possible that the final state may not remain parallel to the initial state. The loss of the parallelity is measured by the geometric phase, as explained here. By expanding the left-hand side of Eq. (9) and noticing that  $\langle\Psi(t)|\frac{d}{dt}|\Psi(t)\rangle dt$  is imaginary, the parallel-transport condition is equivalent to

$$\langle\Psi(t)|\frac{d}{dt}|\Psi(t)\rangle = 0. \quad (10)$$

We rewrite  $|\Psi(t)\rangle$  as  $|\Psi(t)\rangle = e^{i\theta(t)}|\psi(t)\rangle$ , where  $\theta(t)$  contains the information about the phase, including the dynamic and geometric components. However, the parallel-transport condition only allows the geometric phase to survive. Explicitly, if  $|\Psi(t)\rangle$  experiences a dynamic evolution described by  $i\frac{d}{dt}|\Psi(t)\rangle = H|\Psi(t)\rangle$  with  $H$  being the Hamiltonian of a Hermitian quantum system, the condition (10) indicates  $\int_0^t dt' \langle\Psi(t')|H|\Psi(t')\rangle = 0$ , i.e., the dynamic phase vanishes instantaneously. On the other hand, dynamical evolution may also disrupt the parallelity between quantum states and violate the parallel-transport condition. Substituting  $|\Psi(t)\rangle = e^{i\theta(t)}|\psi(t)\rangle$  into the parallel-transport condition, we get

$$i\dot{\theta} + \langle\psi(t)|\frac{d}{dt}|\psi(t)\rangle = 0. \quad (11)$$

In a cyclic process of duration  $\tau$ , the solution to Eq. (11) is the geometric phase

$$\theta(\tau) = i \int_0^\tau dt \langle\psi(t)|\frac{d}{dt}|\psi(t)\rangle. \quad (12)$$

In essence, the parallel-transport condition allows us to separate the total phase into the dynamic and geometric phases. The same formalism also applies to the Aharonov-Anandan phase since  $|\psi(t)\rangle$  here may be either an instantaneous eigenstate of  $H$  or a generic linear combination of the eigenstates of  $H$ .

## 2. Thermal states

The geometric-phase formalism can be generalized to mixed quantum states undergoing a unitary evolution [47]. When a density matrix evolves as  $\rho(t) = U(t)\rho(0)U^\dagger(t)$  with a unitary  $U(t)$ , it acquires a phase  $\theta(t) = \arg \text{Tr}[\rho(0)U(t)]$ . Here “Tr” is the ordinary trace in the Hermitian quantum system. It can be shown that  $\rho(t+dt) = U(t+dt)U^\dagger(t)\rho(t)U(t)U^\dagger(t+dt)$ , yielding that  $\rho(t)$  evolves into  $\rho(t+dt)$  via  $U(t+dt)U^\dagger(t)$ . Accordingly, the condition  $\arg \text{Tr}[\rho(t)U(t+dt)U^\dagger(t)] = 0$  means that  $\rho(t+dt)$  is “in phase” with  $\rho(t)$  since no extra phase is accumulated during the evolution. Taking the differential form, we obtain the parallel-transport condition

$$\text{Tr}[\rho(t)\dot{U}(t)U^\dagger(t)] = \text{Tr}[\rho(0)U^\dagger(t)\dot{U}(t)] = 0. \quad (13)$$

Under this condition,

$$\theta_G(t) = \arg \text{Tr}[\rho(0)U(t)] \quad (14)$$

is the interferometric geometric phase (IGP), introduced in Ref. [47]. Similar to its pure-state counterpart, the parallel-transport condition (13) also prevents the accumulation of the dynamic phase. If  $U(t)$  represents a dynamic evolution, then  $i\dot{U} = HU$ , or equivalently,  $H = i\dot{U}U^\dagger$ . Thus, the dynamic phase accumulated during this evolution vanishes identically:

$$\begin{aligned} \theta_D(t) &= - \int_0^t dt' \text{Tr}[\rho(t')H(t')] \\ &= -i \int_0^t dt' \text{Tr}[\rho(t')\dot{U}(t')U^\dagger(t')] = 0. \end{aligned} \quad (15)$$

If the trace is evaluated with the eigenstates  $\{|n(t)\rangle\}$  of  $\rho(t)$ , only the diagonal elements  $\langle n(t)|U(t)|n(t)\rangle$  are relevant to the determination of  $\theta_G(t)$ . Thus, to specify  $U(t)$ , it was suggested by Sjöqvist *et al.* [47] to strengthen the parallel-transport condition as

$$\langle n(t)|\dot{U}(t)U^\dagger(t)|n(t)\rangle = 0, \quad n = 1, 2, \dots, N. \quad (16)$$

If  $\rho(t)$  is the density matrix of a pure state, Eq. (13) naturally reduces to the condition (10) for pure states.

## III. GEOMETRIC PHASE OF $\mathcal{PT}$ -SYMMETRIC QUANTUM SYSTEMS

### A. Geometric phase for pure states

#### 1. Adiabatic approaches

The concept of the geometric phase has been generalized to some non-Hermitian systems in Ref. [45], where the expression of the Berry phase was obtained by following Berry’s formalism of adiabatic evolution. Explicitly, for a  $\mathcal{PT}$ -symmetric system undergoing evolution along a loop  $C(t) := \mathbf{R}(t)$  with  $0 < t < \tau$  and  $\mathbf{R}(0) = \mathbf{R}(\tau)$  in the parameter manifold, the  $n$ th eigenstate at the end of this evolution is given by

$$|\Psi_n(\mathbf{R}(\tau))\rangle = e^{i\theta_n^D(\tau) + i\theta_n^B(C)} |\Psi_n(\mathbf{R}(0))\rangle. \quad (17)$$

Here,  $\theta_n^D(t) = -\int_0^t dt' E_n(\mathbf{R}(t'))$  represents the instantaneous dynamic phase, and

$$\theta_n^B(C) = i \oint_C d\mathbf{R} \cdot \left[ \langle \Psi_n | W \nabla | \Psi_n \rangle + \frac{1}{2} \langle \Psi_n | (\nabla W) | \Psi_n \rangle \right] \quad (18)$$

is the Berry phase of PTQM following this approach. It should be noted that this result is obtained by beginning with the stationary Schrödinger equation shown in Eq. (2) [45]. In this approach,  $\theta_n^D(t)$  is generated through the time evolution controlled by  $H_0$ , as indicated by Eq. (7).

Meanwhile, a different approach is based on the time evolution described by Eq. (6), whose dynamics is governed by the effective Hamiltonian  $\tilde{H} = H - iS\dot{S}^{-1}$ , with  $S$  being a proper mapping. Different from the prior approach, it will be shown that the ‘‘gauge’’ map  $S$  imparts significant effects on both the dynamic and geometric phases. This also influences the generalization of the geometric phase to thermal states in  $\mathcal{PT}$ -symmetric systems.

When following Eq. (6) along the loop  $C(t)$ , the  $n$ th eigenstate acquires an instantaneous dynamic phase

$$\begin{aligned} \theta_{Dn}^1(t) &= - \int_0^t dt' \langle \Psi_n(t') | W \tilde{H} | \Psi_n(t') \rangle \\ &= - \int_0^t dt' E_n(t') + i \int_0^t dt' \langle \Psi_n^0(t') | \dot{S}^{-1} S | \Psi_n^0(t') \rangle \\ &= \theta_n^D(t) - i \int_0^t dt' \langle \Psi_n^0(t') | S^{-1} \dot{S} | \Psi_n^0(t') \rangle, \end{aligned} \quad (19)$$

where  $|\Psi_n(t)\rangle \equiv |\Psi_n(\mathbf{R}(t))\rangle$  and  $|\Psi_n^0(t)\rangle \equiv |\Psi_n^0(\mathbf{R}(t))\rangle$ . Importantly,  $\theta_n^D(t)$  is real-valued, while  $\theta_{Dn}^1(t)$  is in general complex-valued since the dynamic equation (6) is governed by the non-Hermitian  $\tilde{H}$ . This is reasonable since PTQM may be realized by open systems, and complex phases implies gain or decay of the amplitude. Moreover, the second term in the last line of Eq. (19) is purely imaginary if  $S$  is a proper mapping. To derive the geometric phase, we consider a state  $|\Psi(t)\rangle$  and expand it in terms of the instantaneous eigenstates of  $H(t)$  as

$$|\Psi(t)\rangle = \sum_n c_n(t) e^{i\theta_{Dn}^1(t)} |\Psi_n(t)\rangle. \quad (20)$$

If the system experiences an adiabatic evolution along  $C(t)$ , no level crossing occurs. Thus, we found  $c_n(t) \approx c_n(0) e^{i\theta_n^1(t)}$ , or

$$|\Psi_n(t)\rangle = e^{i\theta_{Dn}^1(t) + i\theta_n^1(t)} |\Psi_n(0)\rangle. \quad (21)$$

Here

$$\theta_n^1(t) = i \int_0^t dt' \langle \Phi_n(t') | \frac{d}{dt'} | \Psi_n(t') \rangle. \quad (22)$$

A detailed derivation is outlined in Appendix B. This definition agrees with some known results [82,83]. Thus, we come to an interesting result: There exist two types of geometric phases in PTQM due to the evolutionary equations associated with the non-Hermitian Hamiltonian and its Hermitian counterpart.

## 2. Parallel-transport conditions

What is the relation between the geometric phases derived previously? Moreover, we have pointed out that there is a more generic way to derive the geometric phase based on the parallelity between quantum states in conventional QM. Does this approach also apply to PTQM? To answer these questions, we first generalize the previously introduced parallel-transport condition to PTQM. Note that the time evolution (6) in a  $\mathcal{PT}$ -symmetric system is controlled by  $H$ , which is related to the Hermitian Hamiltonian  $H_0$  that governs the dynamic equation (7) via a similarity transformation  $S$ .

It has been shown that in conventional QM, the parallel-transport condition (10) ensures that the dynamic phase vanishes. Equivalently, the appearance of a nonvanishing dynamic phase violates the instantaneous parallelity when a state is evolved. Hence, in order to avoid violation of the instantaneous parallelity, we follow an approach similar to that of conventional QM to remove the dynamic phase  $\theta_{Dn}^1$  from Eq. (20) and introduce  $|\tilde{\Psi}_n(t)\rangle = e^{i\theta_n^1(t)} |\Psi_n(t)\rangle$ . Similarly, we also define  $|\tilde{\Psi}_n^0(t)\rangle = e^{i\theta_n^D(t)} |\Psi_n^0(t)\rangle$  by eliminating  $\theta_n^D$  generated during a dynamic evolution controlled by  $H_0$ . A generalizations of Eq. (10) leads to the following parallel-transport (or instantaneous in-phase) conditions:

$$\langle \tilde{\Phi}_n(t) | \frac{d}{dt} | \tilde{\Psi}_n(t) \rangle = 0, \quad (23)$$

$$\langle \tilde{\Psi}_n^0(t) | \frac{d}{dt} | \tilde{\Psi}_n^0(t) \rangle = 0. \quad (24)$$

Thus,  $\theta_n^{1,2}(t)$  is the accumulated phase during the respective parallel transport. Solving these equations, we get

$$\theta_n^1(C) = i \oint_C dt \langle \Phi_n(t) | \frac{d}{dt} | \Psi_n(t) \rangle, \quad (25)$$

$$\theta_n^2(C) = i \oint_C dt \langle \Psi_n^0(t) | \frac{d}{dt} | \Psi_n^0(t) \rangle, \quad (26)$$

at the end of the corresponding parallel transport. Equation (23) reproduces the geometric phase of Eq. (22) derived by the adiabatic approach. Moreover, it can be verified that  $\theta_n^2$  matches the Berry phase shown in Eq. (18):

$$\theta_n^2(C) = \theta_n^B(C) \quad (27)$$

as long as  $S$  is a proper mapping. This is because the adiabatic approach is actually encompassed by the formalism based on parallelity of quantum states.

While Eq. (19) gives a relation between the two dynamic phases  $\theta_{Dn}^1$  and  $\theta_n^D$ , there is a similar relation connecting  $\theta_n^1$  and  $\theta_n^2$ :

$$\theta_n^1 = \theta_n^2 + i \oint dt \langle \Psi_n^0(t) | S^{-1} \dot{S} | \Psi_n^0(t) \rangle. \quad (28)$$

The proofs of Eqs. (27) and (28) are outlined in Appendix B. Interestingly,  $\theta_n^1$  can be complex-valued due to the presence of the non-Hermitian  $\tilde{H}$  in the dynamic evolution (6). Since the dynamic phase  $\theta_{Dn}^1$  is excluded by the parallel-transport condition, what remains is the geometric component  $\theta_n^1$ . As previously noted, the second term in Eq. (28) is purely imaginary if  $S$  is a proper mapping, making  $\theta_n^2$  the real part of  $\theta_n^1$ . Therefore,  $S_{\text{proper}}$  not only connects the Hermitian system governed by  $H^0$  and the  $\mathcal{PT}$ -symmetric system governed by

$H$  but also establishes a link between their geometric phases  $\theta_n^2$  and  $\theta_n^1$ . The imaginary part of  $\theta_n^1$  results in a change of the amplitude of the wave function since the system is non-Hermitian. We will find similar results in our subsequent discussions on thermal states. The relation (28) also yields an interesting result: It is known that the non-Hermitian operator  $S$  acts as a “gauge” to describe how the system interacts with the environment. Apparently,  $\theta_n^1$  is independent of such a gauge, as indicated by Eq. (22), since both  $|\Psi_n\rangle$  and  $|\Phi_n\rangle$  have no dependence on  $H_0$ . However, the real and imaginary parts of  $\theta_n^1$  are determined, respectively, by the proper  $S$ .

In the framework of the IGP, the geometric phase for mixed states is intricately linked to that of pure states. This raises a pertinent question: In the context of PTQM, which one of  $\theta_n^{1,2}$  is more natural for a generalization to thermal states? Referring back to Eqs. (7), (17), and (24), it can be inferred that both  $\theta_n^2$  and  $\theta_n^D$  may arise in a quantum system governed by  $H_0$  if  $S$  is proper. In contrast,  $\theta_n^1$  and  $\theta_{Dn}^1$  can be generated in a  $\mathcal{PT}$ -symmetric system controlled by  $H$ . Consequently, we choose  $\theta_n^1$  and the corresponding approach to develop the formalism of the IGP of thermal states in PTQM.

## B. Interferometric geometric phase for thermal states

### 1. Basic formalism

To generalize the IGP to PTQM, we focus on states in thermal equilibrium at temperature  $T$  described by their non-Hermitian density matrix  $\rho = \frac{1}{Z} e^{-\beta H}$  as stated before. Since the density matrix may be a non-Hermitian operator in those cases, it usually experiences nonunitary evolution since  $H$  is non-Hermitian. We consider a general form  $\rho(t) = U(t)\rho(0)U^{-1}(t)$  with  $\rho(0) = \rho$ . Similar to conventional QM, the system acquires a (total) phase

$$\theta_{\text{tot}}(t) = \arg \text{Tr}[\rho(0)U(t)] \quad (29)$$

during this evolution. Since a statistical ensemble encompasses all energy levels, each weighted by its respective thermal weight, it is more suitable to introduce the geometric phase via the parallel-transport condition, which also fixes the form of  $U(t)$ . To ensure that  $\rho(t + dt)$  is in-phase with  $\rho(t)$  during the evolution, the condition (13) is generalized as

$$\text{Tr}[\rho(t)\dot{U}(t)U^{-1}(t)] = \text{Tr}[\rho(0)U^{-1}(t)\dot{U}(t)] = 0. \quad (30)$$

If  $U(t)$  is a time evolution along a loop in the parameter manifold, then Eq. (6) yields  $i\dot{U} = \tilde{H}U$  or  $i\dot{U}U^{-1} = \tilde{H}$ . Similar to Eq. (15), the parallel-transport condition (30) causes the dynamic phase to vanish:

$$\theta_D(t) = \int_0^t dt' \text{Tr}[\rho(t')\tilde{H}(t')] = 0. \quad (31)$$

This may be realized by choosing a suitable evolution path in the parameter manifold [76]. If the initial density matrix  $\rho(0)$  is given by Eq. (8), the density matrix under parallel-transport evolves as

$$\rho(t) = \sum_n \frac{e^{-\beta E_n}}{Z} |\check{\Psi}_n(t)\rangle\langle\check{\Phi}_n(t)|. \quad (32)$$

Here  $|\check{\Psi}_n(t)\rangle \equiv U(t)|\Psi_n\rangle$  and  $\langle\check{\Phi}_n(t)| = \langle\Phi_n|U^{-1}(t)$ . The trace in Eq. (30) can be evaluated as  $\sum_n \langle\check{\Phi}_n(t)| \cdot |\check{\Psi}_n(t)\rangle$ .

Similar to Eq. (16), the parallel-transport condition is also reinforced as

$$\begin{aligned} \langle\check{\Phi}_n(t)|\dot{U}(t)U^{-1}(t)|\check{\Psi}_n(t)\rangle &= 0, \\ \text{or } \langle\Phi_n|U^{-1}(t)\dot{U}(t)|\Psi_n\rangle &= 0, \quad n = 1, 2, \dots, N. \end{aligned} \quad (33)$$

Since the dynamic phase vanishes during parallel-transport, the system acquires the IGP according to Eq. (29):

$$\theta_G(t) = \theta_{\text{tot}}(t) = \arg \text{Tr}[\rho(0)U(t)]. \quad (34)$$

A transformation satisfying the parallel-transport condition has the form

$$\begin{aligned} U(t) &= \sum_n e^{-\int_0^t \langle\Phi_n(t')|\frac{d}{dt'}|\Psi_n(t')\rangle dt'} |\Psi_n(t)\rangle\langle\Phi_n(0)| \\ &= \sum_n e^{i\theta_n^1(t)} |\Psi_n(t)\rangle\langle\Phi_n(0)|, \end{aligned} \quad (35)$$

where  $|\Psi_n(t)\rangle \equiv |\Psi_n(\mathbf{R}(t))\rangle$  and  $|\Phi_n(t)\rangle \equiv |\Phi_n(\mathbf{R}(t))\rangle$  with  $|\Psi_n(0)\rangle = |\Psi_n\rangle$  and  $|\Phi_n(0)\rangle = |\Phi_n\rangle$ . Thus,  $|\check{\Psi}_n(t)\rangle = e^{i\theta_n^1(t)}|\Psi_n(t)\rangle$ ,  $\langle\check{\Phi}_n(t)| = \langle\Phi_n(t)|e^{-i\theta_n^1(t)}$ , and the parallel-transport condition (33) can also be expressed as

$$\langle\Phi_n(t)|\dot{U}(t)U^{-1}(t)|\Psi_n(t)\rangle = 0, \quad n = 1, 2, \dots, N. \quad (36)$$

Appendix C shows how  $U(t)$  indeed satisfies this condition. Similar to its pure-state counterpart, the dynamic phase  $\theta_{Dn}^1(t)$  for each level is not included to avoid violating the parallel-transport condition. The IGP accumulated during the evolution is

$$\theta_G(t) = \arg \left[ \sum_n \frac{e^{-\beta E_n}}{Z} e^{-\int_0^t \langle\Phi_n(t')|\frac{d}{dt'}|\Psi_n(t')\rangle dt'} v_n(t) \right], \quad (37)$$

where  $v_n(t) = \langle\Phi_n(0)|\Psi_n(t)\rangle$ . If the system undergoes a cyclic process along a loop  $C(t) = \mathbf{R}(t)$  with  $\mathbf{R}(\tau) = \mathbf{R}(0)$ , then  $v_n(\tau) = 1$  and

$$\theta_G(C) = \arg \left[ \sum_n \frac{e^{-\beta E_n}}{Z} e^{i\theta_n^1(C)} \right]. \quad (38)$$

Here  $\theta_n^1(C)$  is the geometric phase factor associated with the  $n$ th individual pure state in the process, given by Eq. (25). It can be shown that  $\theta_G(C)$  reduces to  $\theta_n^1(C)$  in the zero-temperature limit since  $\lim_{\beta \rightarrow \infty} \frac{e^{-\beta E_1}}{Z} = 1$  and  $\lim_{\beta \rightarrow \infty} \frac{e^{-\beta E_{n>1}}}{Z} = 0$ . This is consistent with the reason that we choose  $\theta_n^1(C)$  as the geometric phase for pure states in PTQM. Its effect will be clarified later.

### 2. Generalization to lattice systems

The previous formalism for the IGP is a generalization of the unitary evolution for pure quantum states where the eigenvalues of the Hamiltonian and the density matrix remain unchanged. Therefore, it does not apply to lattice systems with energy bands since the energy now depends on the crystal momentum, which is often treated as a parameter in characterizing the geometry or topology. Fortunately, only a slight modification is needed to extend the previous formalism to lattice systems.

For simplicity, we consider a 1D lattice system where the crystal momentum is denoted by  $k$ . Following the idea of

Ref. [61], the 1D Brillouin zone (BZ) introduces a “transport” of the density matrix

$$\rho(k) = \sum_n \lambda_n(k) |\Psi_n(k)\rangle \langle \Phi(k)|. \quad (39)$$

As a generalization of Eq. (33), if the following condition is satisfied, the eigenstates of  $\rho$  are transported in a parallel manner:

$$\langle \Phi_n(k) | \dot{\Psi}_n(k) \rangle = 0, \quad n = 1, 2, \dots, N, \quad (40)$$

where the derivative is taken with respect to  $k$ . Generically,  $|\Psi_n(k)\rangle$  and  $|\Phi_n(k)\rangle$  do not meet this parallel-transport condition, and we only need to perform the phase shift as

$$\begin{aligned} |\Psi_n(k)\rangle &\rightarrow e^{-\int_0^k \langle \Phi_n(k') | \frac{d}{dk'} |\Psi_n(k')\rangle dk'} |\Psi_n(k)\rangle, \\ \langle \Phi_n(k) | &\rightarrow e^{\int_0^k \langle \Phi_n(k') | \frac{d}{dk'} |\Psi_n(k')\rangle dk'} \langle \Phi_n(k) |, \end{aligned} \quad (41)$$

to ensure that they satisfy Eq. (40) and no other effects will be included. If the transport starts from  $k = 0$ , the system acquires an instantaneous geometric phase

$$\theta_G(k) = \arg \sum_n [\sqrt{\lambda_n(0)\lambda_n(k)} \langle \Phi(0) | \Psi_n(k) \rangle] \quad (42)$$

since the dynamic phase has been eliminated by the parallel-transport condition. If the transport is conducted across the entire Brillouin zone, the periodic condition requires  $\lambda_n(2\pi) = \lambda_n(0)$ , and the results in Sec. III A 2 imply  $|\Psi_n(2\pi)\rangle = e^{i\theta_n^1(\text{BZ})} |\Psi_n(0)\rangle$ . Thus, the IGP that the system acquires at the end of the transport is

$$\begin{aligned} \theta_G(\text{BZ}) &= \arg \sum_n [\lambda_n(0) e^{i\theta_n^1(\text{BZ})}] \\ &= \arg \sum_n \left[ \frac{e^{-\beta E_n(0)}}{Z(0)} e^{i\theta_n^1(\text{BZ})} \right], \end{aligned} \quad (43)$$

which is a direct generalization of Eq. (38) to lattice systems.

#### IV. EXAMPLES

To better understand the IGP of PTQM systems, we investigate two classes of examples exhibiting different IGP behaviors. The first example is fully solvable, allowing for a determination of the proper  $S$  and providing insights into the roles of  $\theta^1$  and  $\theta^2$ . The second one is a  $\mathcal{PT}$ -symmetric band model, which is more relevant to condensed-matter systems. Although the explicit expression of  $S_{\text{proper}}$  for the latter is not readily available, the gauge-independent  $\theta^1$  can still be evaluated. These two examples exhibit significantly different properties. For example, the former demonstrates a temperature-induced geometric phase transition while the latter does not.

##### A. Two-level system

We first study a  $\mathcal{PT}$ -symmetric two-level system introduced in Refs. [45,84] and calculate its IGP. The Hamiltonian is given by

$$H = \epsilon \mathbf{1}_{2 \times 2} + (a \mathbf{n}^r + i b \mathbf{n}^\theta) \cdot \boldsymbol{\sigma}, \quad (44)$$

where  $\boldsymbol{\sigma} = (\sigma_x, \sigma_y, \sigma_z)^T$  is the collection of Pauli matrices, and  $\mathbf{n}^r \equiv (\sin \theta \cos \phi, \sin \theta \sin \phi, \cos \theta)^T$ ,  $\mathbf{n}^\theta \equiv (\cos \theta \cos \phi, \cos \theta \sin \phi, -\sin \theta)^T$  are the unit vectors, respectively, along the radial and tangent directions of a meridian on a unit sphere. The eigenvalues are  $E_{\pm} = \epsilon \pm \sqrt{a^2 - b^2}$ . We limit our discussion to the regime of  $a^2 > b^2$ , where the  $\mathcal{PT}$ -symmetry is preserved and  $E_{\pm}$  are real. Without loss of generality, we let  $a > 0$ . The two eigenvectors are

$$|\Psi_+\rangle = n_+ \begin{pmatrix} (\cos \frac{\theta}{2} - i \alpha \sin \frac{\theta}{2}) e^{-i\phi} \\ i \alpha \cos \frac{\theta}{2} + \sin \frac{\theta}{2} \end{pmatrix}, \quad (45)$$

$$|\Psi_-\rangle = n_- \begin{pmatrix} -(i \alpha \cos \frac{\theta}{2} + \sin \frac{\theta}{2}) e^{-i\phi} \\ \cos \frac{\theta}{2} - i \alpha \sin \frac{\theta}{2} \end{pmatrix}, \quad (46)$$

where  $\alpha = \frac{b}{a + \sqrt{a^2 - b^2}}$  and  $n_{\pm} = e^{-i\frac{\theta}{2}} \sqrt{\frac{a^2 + a\sqrt{a^2 - b^2}}{2(a^2 - b^2)}}$  are normalization coefficients. In the broken  $\mathcal{PT}$ -symmetry phase where  $a^2 \leq b^2$ , it is known that  $\langle \Phi_{\pm} | \Psi_{\pm} \rangle = 0$  [10,85]. Specifically, when  $a^2 = b^2$ ,  $n_{\pm}$  diverges. Thus, the formalism developed for the  $\mathcal{PT}$ -symmetric case breaks down. A full analysis of the broken  $\mathcal{PT}$ -symmetry phase is beyond the scope of the present work. The metric operator  $W$  of this case is

$$W = 1 - \frac{b}{a} \mathbf{n}^\phi \cdot \boldsymbol{\sigma}, \quad (47)$$

where  $\mathbf{n}^\phi = (-\sin \phi, \cos \phi, 0)^T$  is the unit tangent vector of a latitude. In what follows, we will fix  $a$  and  $b$ , thus the parameters  $(\theta, \phi)$  form the parameter manifold  $S^2$ , a unit spherical surface.

Using Eq. (18),  $\theta_{\pm}^2$  associated with a loop  $C$  on  $S^2$  is given by [45]

$$\theta_{\pm}^2(C) = \mp \frac{1}{2} \frac{a}{\sqrt{a^2 - b^2}} \Omega(C) + \left( 1 \pm \frac{a}{\sqrt{a^2 - b^2}} \right) \pi \quad (48)$$

if the north pole is enclosed by  $C$ , or

$$\theta_{\pm}^2(C) = \mp \frac{1}{2} \frac{a}{\sqrt{a^2 - b^2}} \Omega(C) \quad (49)$$

if the north pole is not enclosed by  $C$ . Here  $\Omega(C) = \oint_C d\phi (1 - \cos \theta)$  is the solid angle of the surface enclosed by  $C$  with respect to the origin.

As a concrete example, we take  $a = 3$  and  $b = \sqrt{5}$ , so the eigenvalues become  $E_{\pm} = \epsilon \pm 2$ . To calculate the two terms of  $\theta_{\pm}^1(C)$  via Eq. (28), a proper  $S$  is needed, which may be constructed by solving a differential equation [45]. Details are summarized in Appendix D. Explicitly, it is given by

$$S_{\text{proper}} = \begin{pmatrix} \frac{1}{2} \sqrt{\frac{15}{2}} e^{\frac{i\phi}{4}} & -\frac{1}{2} i \sqrt{\frac{3}{2}} e^{-\frac{5i\phi}{4}} \\ \frac{1}{2} i \sqrt{\frac{3}{2}} e^{\frac{5i\phi}{4}} & \frac{1}{2} \sqrt{\frac{15}{2}} e^{-\frac{i\phi}{4}} \end{pmatrix}. \quad (50)$$

Under this proper transformation, the original non-Hermitian Hamiltonian is converted into a Hermitian one:

$$H_0 = S_{\text{proper}}^{-1} H S_{\text{proper}} = \begin{pmatrix} \epsilon + 2 \cos \theta & 2e^{-\frac{3i\phi}{2}} \sin \theta \\ 2e^{\frac{3i\phi}{2}} \sin \theta & \epsilon - 2 \cos \theta \end{pmatrix}. \quad (51)$$

The eigenvector associated with  $\epsilon + 2$  is

$$|\Psi_+^0(\theta, \phi)\rangle = \begin{pmatrix} \frac{e^{-\frac{5i\phi}{4}} [\cot(\theta) + \csc(\theta)]}{\sqrt{[\cot(\theta) + \csc(\theta)]^2 + 1}} \\ \frac{e^{\frac{i\phi}{4}}}{\sqrt{[\cot(\theta) + \csc(\theta)]^2 + 1}} \end{pmatrix}. \quad (52)$$

It can be shown that

$$\begin{aligned} \langle \Psi_+^0 | S^{-1} dS | \Psi_+^0 \rangle &= -\frac{1}{4} \sqrt{5} \sin \theta d\phi, \\ i \oint_C \langle \Psi_+^0 | S^{-1} \dot{S} | \Psi_+^0 \rangle dt &= -i \frac{\pi}{2} \sqrt{5} \sin \theta, \end{aligned} \quad (53)$$

where the loop  $C$  is chosen as a circle of latitude  $\theta$ . Similarly, the imaginary part of  $\theta_-^1$  is

$$i \oint_C \langle \Psi_-^0 | S^{-1} \dot{S} | \Psi_-^0 \rangle dt = i \frac{\pi}{2} \sqrt{5} \sin \theta. \quad (54)$$

Since the north pole is enclosed by  $C$  (a circle of latitude),  $\theta_{\pm}^2(C)$  is evaluated by Eq. (48). Using Eqs. (28), (48), (53), and (54), the geometric phases associated with the two eigenstates are

$$\begin{aligned} \theta_+^1(C) &= \pi \left( \frac{2 + 3 \cos \theta}{2} \right) - i \frac{\pi}{2} \sqrt{5} \sin \theta, \\ \theta_-^1(C) &= \pi \left( \frac{2 - 3 \cos \theta}{2} \right) + i \frac{\pi}{2} \sqrt{5} \sin \theta, \end{aligned} \quad (55)$$

respectively. Here an extra factor  $2\pi$  is dropped from  $\theta_+^1(C)$ . Accordingly, the IGP is

$$\begin{aligned} \theta_G(C) &= \arg \left[ \frac{e^{-2\beta} e^{i\theta_+^1(C)} + e^{2\beta} e^{i\theta_-^1(C)}}{e^{2\beta} + e^{-2\beta}} \right] \\ &= \arg \left[ e^{-2\beta + \frac{\sqrt{5}\pi}{2} \sin \theta} e^{i\theta_+^2(C)} + e^{2\beta - \frac{\sqrt{5}\pi}{2} \sin \theta} e^{i\theta_-^2(C)} \right], \end{aligned} \quad (56)$$

where  $\theta_{\pm}^2$  is the real part of  $\theta_{\pm}^1$ , as shown by Eq. (28). The imaginary part of  $\theta_{\pm}^1$  actually changes the thermal weight of each energy-level.

Equation (14) shows that the IGP is the argument of  $\text{Tr}[\rho(0)U(t)]$ , which is the ‘‘returning amplitude’’ between the initial state  $\rho(0)$  and the instantaneous state  $\rho(t)$  [47,76]. It can also be thought of as a generalization of the Loschmidt amplitude in mixed quantum states. At its zeros, the IGP exhibits discontinuities and nonanalytical behavior, signaling a change of the geometric nature of the system reflected by the IGP. In this example, the second line of Eq. (56) shows that  $\theta_G(C)$  may become singular if  $\beta = \frac{\sqrt{5}\pi \sin \theta}{4}$ . To examine the IGP of PTQM, we visualize our findings in Figs. 1–3.

In Fig. 1, we present the contour plot of  $\theta_G(C)$  as a function of  $\beta$  and  $\theta$ . On the arc  $\beta = \frac{\sqrt{5}\pi \sin \theta}{4}$ , there are two singular points A and B satisfying  $\theta_{A,B} = \arccos(\pm \frac{1}{3})$ , at which

$$\left[ e^{-2\beta + \frac{\sqrt{5}\pi}{2} \sin \theta} e^{i\theta_+^2(C)} + e^{2\beta - \frac{\sqrt{5}\pi}{2} \sin \theta} e^{i\theta_-^2(C)} \right] \Big|_{\theta=\theta_{A,B}} = 0.$$

Thus, the IGP changes rapidly near A and B according to Eq. (56), indicating discrete jumps of  $\theta_G(C)$  across those singular points. In stark contrast, a jump of the IGP at finite temperature has been ruled out in any two-level model of Hermitian quantum systems [76].

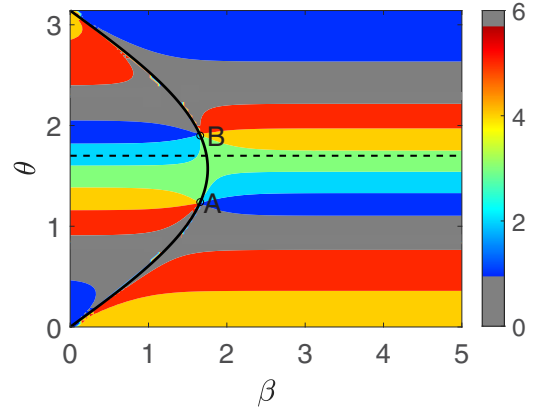


FIG. 1. Contour plot of  $\theta_G(C)$  as a function of  $\beta$  and  $\theta \in [0, \pi]$ , where the range of  $\theta_G(C)$  is within  $[0, 2\pi]$ . The black curve shows the arc  $\beta = \frac{\sqrt{5}\pi \sin \theta}{4}$ , and the value of  $\theta_G(C)$  jumps at the singular points A and B.

To grasp the physical significance of the arc  $\beta = \frac{\sqrt{5}\pi \sin \theta}{4}$ , we revisit the corresponding Hermitian quantum system, where the thermal weight of each level is proportional to  $e^{\mp 2\beta}$  at temperature  $T = \frac{1}{\beta}$ . As  $T \rightarrow 0$ , the relative weight between

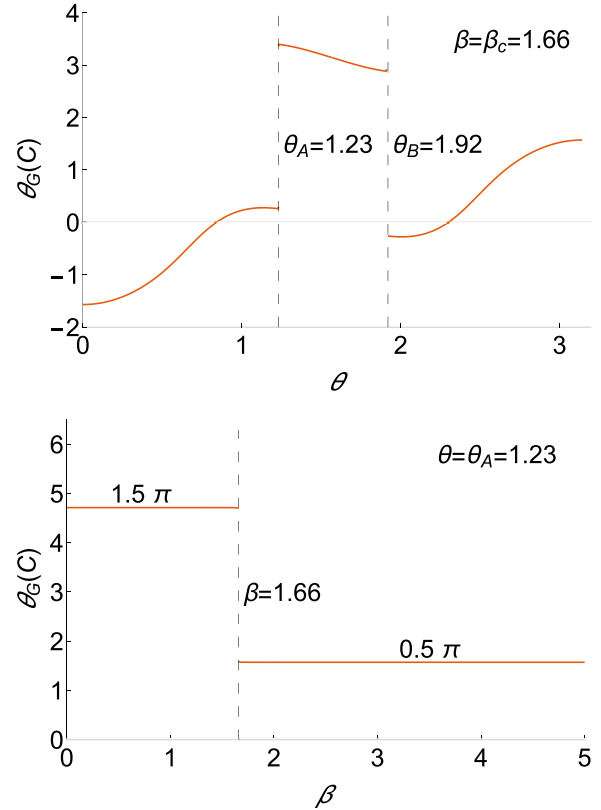


FIG. 2. Top:  $\theta_G(C)$  as a function of  $\theta$  at fixed  $T = \frac{1}{\beta_c}$ . When crossing the singular points  $\theta_A = \arccos(\frac{1}{3}) \doteq 1.23$  and  $\theta_B = \arccos(-\frac{1}{3}) \doteq 1.92$ , there is a  $\pm\pi$ -jump in  $\theta_G(C)$ . Bottom:  $\theta_G(C)$  as a function of  $\beta$  for the evolution along the circle of latitude with  $\theta_A = 1.23$ . As the system crosses the critical inverse temperature  $\beta_c = 1.66$ ,  $\theta_G(C)$  exhibits a  $\pi$ -jump.

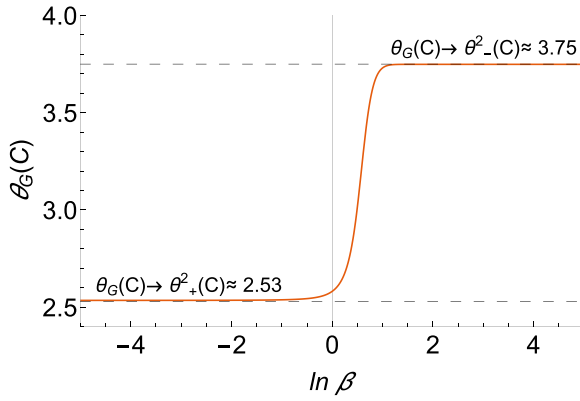


FIG. 3.  $\theta_G(C)$  as a function of  $\ln \beta$  when the system evolves along the circle of latitude  $\theta = 1.7$ , corresponding to the dashed line in Fig. 1. In this case, the imaginary part of  $\theta_{\pm}^1$  has a significant effect on the thermal weights.

the excited and ground states becomes  $\lim_{\beta \rightarrow +\infty} \frac{e^{-2\beta}}{e^{2\beta}} = 0$ , leading the IGP to converge to the geometric phase of the ground state. In the infinite temperature limit ( $\beta \rightarrow 0$ ), the relative weight becomes  $\lim_{\beta \rightarrow 0} \frac{e^{-2\beta}}{e^{2\beta}} = 1$ . In this case, the Hermitian density matrix corresponds to the maximally mixed state, where each level has equal thermal weight, and the IGP loses its resemblance to the ground-state geometric phase. Turning to  $\mathcal{PT}$ -symmetric systems, the parallel-transport condition eliminates the dynamic phase from the total phase, leaving a complex  $\theta_{\pm}^1$ . The imaginary part of  $\theta_{\pm}^1$  modifies the thermal weights of the two levels to  $\exp[\mp(2\beta - \frac{\sqrt{5\pi} \sin \theta}{2})]$ , which will be referred to as the “effective thermal weights.” Notably, in the low-temperature limit, the behavior of the IGP can still mirror that of the corresponding Hermitian system. In Fig. 1, the domain where  $\beta > \frac{\sqrt{5\pi} \sin \theta}{4}$  corresponds to the phase at “effective” positive temperatures for the non-Hermitian quantum system. The arc  $\beta = \frac{\sqrt{5\pi} \sin \theta}{4}$  signifies the “effective” infinite-temperature threshold. Conversely, the regime where  $\beta < \frac{\sqrt{5\pi} \sin \theta}{4}$  corresponds to the phase at “effective” negative temperatures. In this scenario, the original temperature  $T$  along with the imaginary part of  $\theta_{\pm}^1$  determines the relative thermal distribution between the excited and ground states.

At the singular points A and B, the corresponding critical inverse temperature is  $\beta_c = \frac{\sqrt{5\pi} \sin \theta_{A,B}}{4} = 1.66$ . Moreover, Eq. (55) implies

$$\theta_{\pm}^2(\theta_A) - \theta_{\mp}^2(\theta_A) = \pi, \quad \theta_{\pm}^2(\theta_B) - \theta_{\mp}^2(\theta_B) = -\pi. \quad (57)$$

When the system is at temperature  $T_c = \frac{1}{\beta_c}$  and evolves along a circle of latitude  $\theta < \theta_A$ , the system resides in the “effective” positive-temperature region, as it is situated below point A in Fig. 1. In this scenario, the effective thermal weight of the ground state exceeds that of the excited state. Thus,  $\theta_G$  resembles the geometric phase of the ground state,  $\theta^2(\theta)$ . Upon crossing  $\theta_A$  from below, the system with  $\theta > \theta_A$  enters the “effective” negative-temperature regime, causing the relative effective thermal weights of the ground and excited states to reverse. The IGP then begins to resemble the geometric phase of the excited state,  $\theta^2(\theta)$ . According to Eq. (57), the IGP

undergoes a  $\pi$ -jump, indicating that the geometric nature of the evolution along the circle of  $\theta < \theta_A$  is essentially different from that of the evolution along the circle of  $\theta > \theta_A$  at  $T_c$ . Similar phenomena occur when crossing  $\theta_B$  at  $T_c$  as well. The IGP experiences a  $-\pi$ -jump according to Eq. (57). To better visualize the phenomena, we plot the IGP versus the latitude  $\theta$  at  $\beta_c = 1.66$  in the top panel of Fig. 2. The behavior of the IGP totally agrees with the above analysis.

Similarly, the geometric nature of the evolution along a circle of fixed latitude  $\theta = \theta_A$  changes as the inverse temperature crosses  $\beta_c$ . This transition is clearly depicted in the bottom panel of Fig. 2. We refer to this nonanalytical behavior of the IGP as signaling a geometric phase transition. Explicitly, the system at point A is in the “effective” positive-temperature phase when  $\beta > \beta_c$  and the IGP resembles  $\theta_-^2(C) = \frac{\pi}{2}$ , the real-valued geometric phase of the ground state. After crossing  $\beta_c$ , the system enters the “effective” negative-temperature phase with  $\beta < \beta_c$ , and the IGP changes to resemble  $\theta_+^2(C) = -\frac{\pi}{2} \equiv \frac{3\pi}{2} \pmod{2\pi}$ , the real-valued geometric phase of the excited state.

When  $\theta \neq \theta_{A,B}$ , the IGP represents a continuous interpolation between the  $\theta^2$  of the excited and ground states as temperature varies. If  $\theta = \frac{\pi}{2}$ , Eq. (55) implies  $\theta_-^2 = \theta_+^2 = \pi$  and indicates that the IGP is a trivial interpolation. To present a nontrivial interpolation, we choose  $\theta = 1.70$ , which leads to  $\theta_-^2 \approx 3.75$  and  $\theta_+^2 \approx 2.53$ . The behavior of  $\theta_G(C)$  is illustrated in Fig. 3, where  $\beta$  transitions from 0 (the infinite-temperature limit) to  $+\infty$  (the low-temperature limit) displayed on a logarithmic scale. In the scenario in which  $\beta \rightarrow +\infty$ ,  $\theta_G(C) \rightarrow \theta_-^2(C)$ . Conversely, when  $\beta$  approaches 0,  $\theta_G(C)$  approximates  $\theta_+^2(C)$ .

### B. 1D $\mathcal{PT}$ -symmetric Su-Schrieffer-Heeger model

Our second example investigates a spatially periodic system, namely the bipartite dissipative model with staggered imaginary on-site potentials and alternating hopping parameters [86] inspired by the Su-Schrieffer-Heeger (SSH) model [87]. The Hamiltonian can be written as

$$H = \sum_m [\varepsilon_A c_m^\dagger c_m + \varepsilon_B d_m^\dagger d_m + v(c_m^\dagger d_m + d_m^\dagger c_m) + v'(c_m^\dagger d_{m+1} + d_{m+1}^\dagger c_m)]. \quad (58)$$

Here, A and B are the two sites of the  $m$ th cell,  $\varepsilon_A$  and  $\varepsilon_B = \varepsilon_A - 2i\Gamma$  are the associated on-site energies with  $\Gamma$  denoting the imaginary potential, and  $v$  and  $v'$  are the intracell and intercell hopping coefficients, respectively. The Hamiltonian with a periodic boundary condition can be cast into the Bloch form

$$H = \sum_k (c_k^\dagger, d_k^\dagger) \begin{bmatrix} \varepsilon_A & v_k \\ v_k^* & \varepsilon_B \end{bmatrix} \begin{pmatrix} c_k \\ d_k \end{pmatrix}, \quad (59)$$

where  $v_k = v + v'e^{ik}$ . We will set  $\varepsilon_A = -\varepsilon_B = i\Gamma$  to symmetrize the on-site potentials. Introducing  $\cos \phi_k \equiv \frac{i\Gamma}{\sqrt{|v_k|^2 - \Gamma^2}}$ , which is a complex trigonometric function, the eigenvalues



and eigenstates of  $H$  and  $H^\dagger$  are given as follows:

$$\begin{aligned}
 E_\pm(k) &= \pm\sqrt{|v_k|^2 - \Gamma^2}, \\
 |\Psi_+\rangle &= \begin{pmatrix} \frac{v_k}{|v_k|} \cos \frac{\phi_k}{2} \\ \sin \frac{\phi_k}{2} \end{pmatrix}, |\Psi_-\rangle = \begin{pmatrix} -\frac{v_k}{|v_k|} \sin \frac{\phi_k}{2} \\ \cos \frac{\phi_k}{2} \end{pmatrix}, \\
 |\Phi_+\rangle &= \begin{pmatrix} \frac{v_k}{|v_k|} \cos^* \frac{\phi_k}{2} \\ \sin^* \frac{\phi_k}{2} \end{pmatrix}, |\Phi_-\rangle = \begin{pmatrix} -\frac{v_k}{|v_k|} \sin^* \frac{\phi_k}{2} \\ \cos^* \frac{\phi_k}{2} \end{pmatrix}. \quad (60)
 \end{aligned}$$

If  $|v_k|^2 > \Gamma^2$ , the model is in  $\mathcal{PT}$ -symmetric phase and  $E_\pm(k)$  is real-valued. Using Eq. (22), the Berry phase for each energy level associated with the first Brillouin zone is

$$\theta_\pm^1(\text{BZ}) = i \int_{\text{BZ}} \langle \Phi_\pm | \frac{\partial}{\partial k} | \Psi_\pm \rangle dk. \quad (61)$$

Introducing the parameters  $q = \frac{v'}{v}$ ,  $\eta = \frac{\Gamma}{v}$ ,  $x = \frac{4q}{(q+1)^2}$ , and  $y = \frac{4q}{(q+1)^2 - \eta^2}$  and following Ref. [83], the expression of  $\theta_\pm^1$  becomes

$$\begin{aligned}
 \theta_\pm^1(\text{BZ}) &= \pi \Theta(q - 1) \\
 &\pm \frac{i\eta}{\sqrt{(q+1)^2 - \eta^2}} \left[ K(y) + \frac{q-1}{q+1} \Pi(x, y) \right]. \quad (62)
 \end{aligned}$$

Here  $\Theta(q - 1)$  is the step function, and

$$\begin{aligned}
 K(y) &= \int_0^{\frac{\pi}{2}} \frac{dk}{\sqrt{1 - y \sin^2 k}}, \\
 \Pi(x, y) &= \int_0^{\frac{\pi}{2}} \frac{dk}{(1 - x \sin^2 k) \sqrt{1 - y \sin^2 k}} \quad (63)
 \end{aligned}$$

are elliptic integrals. The presence of those integrals makes it difficult to derive an analytic expression for  $S_{\text{proper}}$ . Nevertheless,  $\theta_\pm^2$  can still be obtained by extracting the real part of  $\theta_\pm^1$ , as previously mentioned. When  $q$  changes from  $1^-$  to  $1^+$ , the value of  $\theta_\pm^2$  experiences a  $\pi$ -jump due to the step function, which is similar to the well-known result of the Hermitian SSH model [88], as the topological structure of the energy bands changes.

If  $|v_k|^2 < \Gamma^2$ , the system is in the broken  $\mathcal{PT}$ -symmetry regime, rendering the previous formalism inapplicable. Utilizing the previously introduced parameters, the condition for preserving  $\mathcal{PT}$ -symmetry can be expressed as  $1 + 2q \cos k + q^2 > \eta^2$ , implying

$$(q+1)^2 - \eta^2 > 2q(1 - \cos k) \geq 4q, \quad (64)$$

which is equivalent to  $0 < y < 1$  (note that  $q > 0$ ). In this case, the elliptic integrals in Eq. (63) are both real-valued. Accordingly, Eq. (62) indicates that  $\theta_\pm^2(\text{BZ}) = \text{Re}\theta_\pm^1(\text{BZ}) = \pi \Theta(q - 1)$ . Solving the inequality  $y > 1$ , we get the broken  $\mathcal{PT}$ -symmetry regime on the  $(q, \eta)$ -plane determined by  $1 < q < \eta + 1$  or  $1 - \eta < q < 1$ . In this case, the elliptic integrals in Eq. (63) become singular since  $1 - y \sin^2 k$  has zero points.

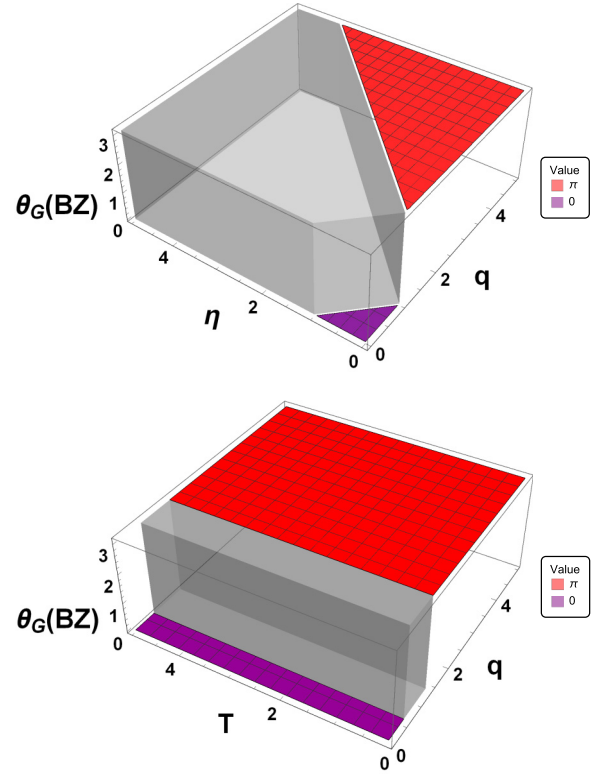


FIG. 4. Top: Plot of the IGP in the  $(q, \eta)$ -plane. The gray region represents the  $\mathcal{PT}$ -broken symmetry phase. In the  $\mathcal{PT}$ -symmetric regions where  $q + \eta < 1$  and  $q > \eta + 1$ , the value of  $\theta_G(\text{BZ})$  is 0 and  $\pi$ , respectively. At the point  $(q, \eta) = (1, 0)$ , the IGP experiences a  $\pi$ -jump. Bottom: Plot of the IGP in the  $(q, T)$ -plane with  $\eta = 0.3$ . The region where  $0.7 < q < 1.3$  represents the  $\mathcal{PT}$ -broken symmetry phase, which crosses the  $q = 1$  line. Similarly, in the two  $\mathcal{PT}$ -symmetric regions where  $q < 0.7 = 1 - \eta$  and  $q > 1.3 = 1 + \eta$ , the value of the IGP is 0 and  $\pi$ , respectively.

According to Eq. (43), the IGP of the  $\mathcal{PT}$ -symmetric SSH model is

$$\begin{aligned}
 \theta_G(\text{BZ}) &= \arg \left[ \frac{e^{-\beta E_+(0)} e^{i\theta_+^1(\text{BZ})} + e^{-\beta E_-(0)} e^{i\theta_-^1(\text{BZ})}}{e^{-\beta E_+(0)} + e^{-\beta E_-(0)}} \right] \\
 &= \arg \left[ e^{-\beta E_+(0) - \text{Im}\theta_+^1} e^{i\theta_+^2} + e^{-\beta E_-(0) - \text{Im}\theta_-^1} e^{i\theta_-^2} \right] \\
 &= \arg \left[ (e^{\beta E_-(0) + \text{Im}\theta_-^1} + e^{-\beta E_-(0) - \text{Im}\theta_-^1}) e^{i\theta_-^2} \right] \\
 &= \theta_-^2, \quad (65)
 \end{aligned}$$

where the label “BZ” is suppressed after the second line for simplicity, and  $E_+ = -E_-$ ,  $\text{Im}\theta_+^1 = -\text{Im}\theta_-^1$ , and  $\theta_+^2 = \theta_-^2$  (since  $\pi = -\pi \pmod{2\pi}$ ) have been applied. Unlike the first example, in the  $\mathcal{PT}$ -symmetric phase, the IGP of the SSH model is equal to the real-valued geometric phase  $\theta^2$  of the ground state and independent of temperature. Consequently, the IGP in this model cannot probe any geometric phase transition induced by temperature. However, it inherits the same topological properties as the geometric phase for pure states, meaning it can detect the same geometric phase transition induced by  $q$  and  $\eta$  as  $\theta^2$  does.

Figure 4 illustrates the behavior of  $\theta_G$  on the  $(q, \eta)$ - and  $(q, T)$ -planes, respectively. In the top panel, the IGP is plotted

in the  $\mathcal{PT}$ -symmetric regions with  $q + \eta < 1$  and  $q > \eta + 1$ . The point  $(q, \eta) = (1, 0)$  is the gapless point where the geometric phase jumps. The IGP in the two  $\mathcal{PT}$ -symmetric regions takes the values 0 and  $\pi$ , respectively. Therefore, the IGP is constant within the same  $\mathcal{PT}$ -symmetric region but differs from the IGP on the other region. In the bottom panel, we plot the IGP in the  $(q, T)$ -plane when  $\eta = 0.3$ . At finite temperatures, the IGP exhibits the same features of the geometric phase for pure states: Its values are, respectively, 0 and  $\pi$  in the two  $\mathcal{PT}$ -symmetric regions. However, the broken  $\mathcal{PT}$ -symmetry region separates the two regions. Thus, the IGP from the  $\mathcal{PT}$ -symmetric formalism is disrupted. Nevertheless, the IGP reveals the different geometric phases as  $q$  and  $\eta$  vary. For the  $\mathcal{PT}$ -symmetric SSH model studied here, the independence of the IGP with respect to temperature allows the determination of  $\theta^2$  at zero temperature even when the system is at finite temperature.

### C. Implications

On the one hand, PTQM may be realized in driven systems. For example, Ref. [89] demonstrated a  $\mathcal{PT}$ -symmetric quantum system with two coupled optical waveguides selectively pumped. By modulating the refractive index along the waveguides, the Hamiltonian may be engineered to the desired form. On the other hand, the IGP of mixed states in Hermitian systems has been measured by using a Mach-Zehnder interferometer setup demonstrated in Refs. [62,65], where mixed states were generated through two methods: Decohering pure states with birefringent elements, and creating a non-maximally-entangled state of two photons followed by tracing out one photon.

As shown in this work, the IGP of PTQM is in general complex-valued, where the real part represents a phase factor while the imaginary part adjusts the distribution. By applying the phase measurement [62,65] to extract the IGP of mixed states in  $\mathcal{PT}$ -symmetric systems, it is likely we will extract only the thermal average of the IGPs of individual states. Nevertheless, one may compare the population distribution of the evolved system with that of a corresponding system without the accumulation of the IGP. The difference in the distribution is due to the imaginary part of the IGP of the PTQM system. Therefore, the real and imaginary parts of the IGP of PTQM systems seem to be measurable, even though the procedure is more complicated due to the lack of Hermiticity.

## V. CONCLUSION

The concept of the geometric phase has been generalized to PTQM via the introduction of parallel-transport. For pure-states, the parallel-transport conditions for the eigenstates of  $H$  and  $H_0$  lead to distinct generalizations of the geometric phases,  $\theta^1$  and  $\theta^2$ , as obtained by conventional methods. In general,  $\theta^1$  is complex and  $\theta^2$  is its real part. As  $\theta^1$  arises from the non-Hermitian Hamiltonian, it is generalized to mixed states in PTQM. Moreover, the discussion of the IGP of mixed states is meaningful after the dynamic phase has been removed by the parallel-transport condition. The imaginary part of the IGP of PTQM affects the thermal weights and introduces effective temperatures. Consequently, even in a

simple two-level system, the IGP of PTQM can display interesting behaviors unavailable in conventional QM, such as the geometric phase transition of a two-level system at finite temperature. For more complicated non-Hermitian quantum systems, the generalized IGP may serve as a probe to uncover intriguing characteristics due to geometry and topology.

## ACKNOWLEDGMENTS

H.G. was supported by the National Natural Science Foundation of China (Grant No. 12074064) and the Innovation Program for Quantum Science and Technology (Grant No. 2021ZD0301904). X.Y.H. was supported by the Jiangsu Funding Program for Excellent Postdoctoral Talent (Grant No. 2023ZB611). C.C.C. was supported by the National Science Foundation under Grant No. PHY-2310656

## APPENDIX A: DYNAMIC EQUATION OF $|\Psi^0\rangle$

Recalling that  $H = SH_0S^{-1}$  and  $|\Psi^0\rangle = S^{-1}|\Psi\rangle$ , we substitute them into Eq. (5) and get

$$\begin{aligned} i\frac{d}{dt}(S|\Psi^0\rangle) &= i\dot{S}|\Psi^0\rangle + iS\frac{d}{dt}|\Psi^0\rangle \\ &= H - \frac{i}{2}SS^\dagger[(\dot{S}^{-1})^\dagger S^{-1} + (S^{-1})^\dagger \dot{S}^{-1}]S|\Psi^0\rangle \\ &= \left\{ HS - \frac{i}{2}[SS^\dagger(\dot{S}^{-1})^\dagger + S\dot{S}^{-1}S] \right\}|\Psi^0\rangle. \end{aligned} \quad (\text{A1})$$

After moving the first term  $i\dot{S}|\Psi^0\rangle$  to the right-hand side and left-multiplying  $S^{-1}$  on both sides, we obtain the dynamic equation of  $|\Psi^0\rangle$ :

$$i\frac{d}{dt}|\Psi^0\rangle = \left\{ H_0 + \frac{i}{2}[\dot{S}^{-1}S - S^\dagger(\dot{S}^{-1})^\dagger] \right\}|\Psi^0\rangle. \quad (\text{A2})$$

If  $S$  is a proper mapping satisfying

$$\dot{S}_{\text{proper}}^{-1}S_{\text{proper}} = (\dot{S}_{\text{proper}}^{-1}S_{\text{proper}})^\dagger, \quad (\text{A3})$$

the dynamic equation  $|\Psi^0\rangle$  reduces to Eq. (7), the ordinary Schrödinger equation. Thus, the time-dependent PTQM is “mapped to” the conventional QM by  $S_{\text{proper}}$ .

## APPENDIX B: DETAILS OF THE GEOMETRIC PHASE OF PURE STATES

To derive the geometric phase shown in Eq. (22), the expansion (20) is plugged into Eq. (6), yielding

$$i|\dot{\Psi}\rangle = \sum_m [(i\dot{c}_m + c_m\tilde{E}_m)e^{i\theta_{0m}^1}|\Psi_m\rangle + c_me^{i\theta_{0m}^1}|\dot{\Psi}_m\rangle], \quad (\text{B1})$$

where  $\tilde{E}_m = E_m + i\langle\Psi_m^0|S^{-1}\dot{S}|\Psi_m^0\rangle$ . Applying Eq. (6), the left-hand side becomes

$$i|\dot{\Psi}\rangle = \sum_m c_me^{i\theta_{0m}^1}(E_m - iS\dot{S}^{-1})|\Psi_m\rangle. \quad (\text{B2})$$

Multiplying the above equations by  $\langle\Phi_n|$  from the left and applying the relation [45]

$$\langle\Phi_n|\dot{\Psi}_m\rangle = \frac{\langle\Phi_n|\dot{H}|\Psi_m\rangle}{E_n - E_m} \text{ for } m \neq n, \quad (\text{B3})$$

we get

$$\begin{aligned} \dot{c}_n &= ic_n \langle \Phi_n | \dot{\Psi}_n \rangle \\ &+ i \sum_{m \neq n} c_m e^{i(\theta_{D_m}^1 - \theta_{D_n}^1)} \langle \Phi_n | \left( \frac{\dot{H}}{E_n - E_m} + iS\dot{S}^{-1} \right) | \Psi_m \rangle. \end{aligned} \quad (\text{B4})$$

As in conventional quantum mechanics, the adiabatic approximation is employed, so level-crossing terms (i.e., terms with  $m \neq n$ ) are dropped. We finally get

$$\dot{c}_n(t) \doteq ic_n(t) \langle \Phi_n | \frac{d}{dt} | \Psi_n \rangle, \quad (\text{B5})$$

whose solution is

$$c_n(t) \approx c_n(0) e^{-\int_0^t dt' \langle \Phi_n(t') | \frac{d}{dt'} | \Psi_n(t') \rangle}. \quad (\text{B6})$$

Next, we verify that

$$\begin{aligned} \theta_n^2(\tau) &= i \oint_C dt \langle \Psi_n^0(t) | \frac{d}{dt} | \Psi_n^0(t) \rangle \\ &= i \oint_C d\mathbf{R} \cdot \left[ \langle \Psi_n | W \nabla | \Psi_n \rangle + \frac{1}{2} \langle \Psi_n | (\nabla W) | \Psi_n \rangle \right] \\ &= \theta_n^B \end{aligned} \quad (\text{B7})$$

subject to  $\dot{S}^{-1}S = (\dot{S}^{-1}S)^\dagger$ . Using  $|\Phi_n(t)\rangle = W(t)|\Psi_n(t)\rangle$  and  $W^\dagger = W$ , the first term on the right-hand side of Eq. (18) is simply  $\theta_n^1$ , which can be further expressed as

$$\begin{aligned} \theta_n^1 &= i \oint dt \langle \Phi_n(t) | \frac{d}{dt} | \Psi_n(t) \rangle \\ &= i \oint dt \langle \Psi_n^0(t) | S^{-1} \dot{S} | \Psi_n^0(t) \rangle + i \oint dt \langle \Psi_n^0(t) | \frac{d}{dt} | \Psi_n^0(t) \rangle \\ &= i \oint dt \langle \Psi_n^0(t) | S^{-1} \dot{S} | \Psi_n^0(t) \rangle + \theta_n^2. \end{aligned} \quad (\text{B8})$$

The second term on the right-hand side of Eq. (18) is

$$\begin{aligned} &\frac{i}{2} \oint_C \langle \Psi_n(t) | \dot{W} | \Psi_n(t) \rangle dt, \\ &= \frac{i}{2} \oint_C \langle \Psi_n(t) | (\dot{S}^{-1})^\dagger S^{-1} + (S^{-1})^\dagger \dot{S}^{-1} | \Psi_n(t) \rangle dt, \\ &= \frac{i}{2} \oint_C \langle \Psi_n^0(t) | [S^\dagger (\dot{S}^{-1})^\dagger + \dot{S}^{-1} S] | \Psi_n^0(t) \rangle dt, \\ &= -i \oint_C \langle \Psi_n^0(t) | S^{-1} \dot{S} | \Psi_n^0(t) \rangle dt, \end{aligned} \quad (\text{B9})$$

where we have applied  $S^\dagger (\dot{S}^{-1})^\dagger = \dot{S}^{-1} S$  from the proper mapping condition. Along with Eq. (B8), we conclude that  $\theta_n^B = \theta_n^2$ .

### APPENDIX C: DETAILS OF GEOMETRIC PHASE OF THERMAL STATES

To verify that  $U(t)$  in Eq. (35) satisfies the parallel-transport condition (33), we need the following

identities:

$$\begin{aligned} \dot{U}(t) &= - \sum_n \langle \Phi_n(t) | \frac{d}{dt} | \Psi_n(t) \rangle U(t) \\ &+ \sum_n e^{-\int (\Phi_n(t') | \frac{d}{dt'} | \Psi_n(t') \rangle dt'} \left( \frac{d}{dt} | \Psi_n(t) \rangle \right) \langle \Phi_n(0) |, \\ U^{-1}(t) &= \sum_n e^{\int (\Phi_n(t') | \frac{d}{dt'} | \Psi_n(t') \rangle dt'} | \Psi_n(0) \rangle \langle \Phi_n(t) |. \end{aligned}$$

They lead to Eq. (33):

$$\begin{aligned} &\langle \Phi_n(t) | \dot{U}(t) U^{-1}(t) | \Psi_n(t) \rangle \\ &= \langle \Phi_n(t) | \left[ - \langle \Phi_n(t) | \frac{d}{dt} | \Psi_n(t) \rangle \right. \\ &\quad \left. + \left( \frac{d}{dt} | \Psi_n(t) \rangle \right) \langle \Phi_n(t) | \right] | \Psi_n(t) \rangle \\ &= - \langle \Phi_n(t) | \frac{d}{dt} | \Psi_n(t) \rangle + \langle \Phi_n(t) | \frac{d}{dt} | \Psi_n(t) \rangle \\ &= 0. \end{aligned} \quad (\text{C1})$$

Note that  $\int (\Phi_n(t') | \frac{d}{dt'} | \Psi_n(t') \rangle dt'$  is complex in general, so  $U^{-1} \neq U^\dagger$  in general. Thus,  $U$  does not necessarily represent a unitary evolution.

### APPENDIX D: PROPER MAPPING OF THE TWO-LEVEL SYSTEM

To search for a proper mapping  $S$  of our example in the main text, we first notice that  $W = (S^{-1})^\dagger S^{-1}$ , which is invariant under a  $U(N)$  transformation  $u$ :  $S'^{-1} = uS^{-1} \rightarrow W = (S'^{-1})^\dagger S'^{-1}$ . We can use this degree of freedom to obtain a proper  $S$ . For convenience, we initially take  $W = (S^{-1})^2$  or conversely  $S^{-1} = \sqrt{W}$  since  $W$  is already given by Eq. (47). Since  $W$  is Hermitian, this kind of  $S$  has at least two solutions:

$$S_{\pm}^{-1} = \frac{\begin{pmatrix} \sqrt{a^2 - b^2} \pm a & ibe^{-i\tau} \\ -ibe^{i\tau} & \sqrt{a^2 - b^2} \pm a \end{pmatrix}}{\sqrt{2a(\sqrt{a^2 - b^2} \pm a)}}. \quad (\text{D1})$$

Take  $a = 3$  and  $b = \sqrt{5}$  and choose  $S = S_+$  without loss of generality. Then

$$S = \begin{pmatrix} \frac{\sqrt{\frac{15}{2}}}{2} & -\frac{1}{2}i\sqrt{\frac{3}{2}}e^{-i\phi} \\ \frac{1}{2}i\sqrt{\frac{3}{2}}e^{i\phi} & \frac{\sqrt{\frac{15}{2}}}{2} \end{pmatrix} \quad (\text{D2})$$

and the original Hamiltonian is converted to

$$H_0 = S^{-1} H S = \begin{pmatrix} \epsilon + 2 \cos \theta & 2e^{-i\phi} \sin \theta \\ 2e^{i\phi} \sin \theta & \epsilon - 2 \cos \theta \end{pmatrix}. \quad (\text{D3})$$

The eigenvector of  $H_0$  associated with  $E_+ = \epsilon + 2$  is

$$|\Psi_+^0(\theta, \phi)\rangle = \begin{pmatrix} \frac{e^{-i\phi} (\cot \theta + \csc \theta)}{\sqrt{(\cot \theta + \csc \theta)^2 + 1}} \\ \frac{1}{\sqrt{(\cot \theta + \csc \theta)^2 + 1}} \end{pmatrix}, \quad (\text{D4})$$

which leads to

$$\begin{aligned} \langle \Psi_+^0 | S^{-1} dS | \Psi_+^0 \rangle &= -\frac{1}{4}(\sqrt{5} \sin \theta + i \cos \theta) d\phi, \\ i \oint_C \langle \Psi_+^0 | S^{-1} dS | \Psi_+^0 \rangle dt &= \frac{\pi}{2}(\cos \theta - i\sqrt{5} \sin \theta). \end{aligned} \quad (\text{D5})$$

Apparently, the second term of  $\theta_+^1$  is complex in this case. To make it purely imaginary, we impose a unitary transformation  $S^{-1} = uS_{\text{proper}}^{-1}$ , where  $u$  can be fixed by the condition of a proper mapping  $\dot{S}_{\text{proper}}^{-1} S_{\text{proper}} = (\dot{S}_{\text{proper}}^{-1} S_{\text{proper}})^\dagger$ . This is equivalent to solving the equation

$$\dot{u} = \frac{1}{2}[\dot{S}^{-1}S - (\dot{S}^{-1}S)^\dagger]u \quad (\text{D6})$$

subject to the initial condition  $u(0) = \mathbf{1}_{2 \times 2}$ . The general solution is quite involved. Fortunately, if the system evolves along a circle of latitude such that  $d\theta = 0$ , an analytical expression of  $u$  can be found as

$$u(\phi) = \begin{pmatrix} e^{\frac{i\phi}{4}} & 0 \\ 0 & e^{-\frac{i\phi}{4}} \end{pmatrix}. \quad (\text{D7})$$

Accordingly, the proper mapping  $S$  is

$$S_{\text{proper}} = Su = \begin{pmatrix} \frac{1}{2}\sqrt{\frac{15}{2}}e^{\frac{i\phi}{4}} & -\frac{1}{2}i\sqrt{\frac{3}{2}}e^{-\frac{5i\phi}{4}} \\ \frac{1}{2}i\sqrt{\frac{3}{2}}e^{\frac{5i\phi}{4}} & \frac{1}{2}\sqrt{\frac{15}{2}}e^{-\frac{i\phi}{4}} \end{pmatrix}. \quad (\text{D8})$$

- 
- [1] H. Feshbach, Unified theory of nuclear reactions, *Ann. Phys.* **5**, 357 (1958).
- [2] N. Moiseyev, *Non-Hermitian Quantum Mechanics* (Cambridge University Press, Cambridge, UK, 2011).
- [3] R. El-Ganainy, K. G. Makris, M. Khajavikhan, Z. H. Musslimani, S. Rotter, and D. N. Christodoulides, Non-Hermitian physics and PT symmetry, *Nat. Phys.* **14**, 11 (2018).
- [4] N. Hatano and D. R. Nelson, Localization transitions in non-Hermitian quantum mechanics, *Phys. Rev. Lett.* **77**, 570 (1996).
- [5] N. Matsumoto, K. Kawabata, Y. Ashida, S. Furukawa, and M. Ueda, Continuous phase transition without gap closing in non-Hermitian quantum many-body systems, *Phys. Rev. Lett.* **125**, 260601 (2020).
- [6] Z. Gong, M. Bello, D. Malz, and F. K. Kunst, Anomalous behaviors of quantum emitters in non-Hermitian baths, *Phys. Rev. Lett.* **129**, 223601 (2022).
- [7] F. Roccati, S. Lorenzo, G. Calajò, G. M. Palma, A. Carollo, and F. Ciccarello, Exotic interactions mediated by a non-Hermitian photonic bath, *Optica* **9**, 565 (2022).
- [8] B. Liegeois, C. Ramasubramanian, and N. Defenu, Tunable tachyon mass in the  $PT$ -broken massive Thirring model, *Phys. Rev. D* **108**, 116014 (2023).
- [9] L. Lamata, J. León, T. Schätz, and E. Solano, Dirac equation and quantum relativistic effects in a single trapped ion, *Phys. Rev. Lett.* **98**, 253005 (2007).
- [10] Z. Gong, Y. Ashida, K. Kawabata, K. Takasan, S. Higashikawa, and M. Ueda, Topological phases of non-Hermitian systems, *Phys. Rev. X* **8**, 031079 (2018).
- [11] F. K. Kunst, E. Edvardsson, J. C. Budich, and E. J. Bergholtz, Biorthogonal bulk-boundary correspondence in non-Hermitian systems, *Phys. Rev. Lett.* **121**, 026808 (2018).
- [12] F. Roccati, M. Bello, Z. Gong *et al.*, Hermitian and non-Hermitian topology from photon-mediated interactions, *Nat. Commun.* **15**, 2400 (2024).
- [13] C. M. Bender and S. Boettcher, Real spectra in non-Hermitian hamiltonians having  $\mathcal{PT}$  symmetry, *Phys. Rev. Lett.* **80**, 5243 (1998).
- [14] G. L. Giorgi, Spontaneous  $\mathcal{PT}$  symmetry breaking and quantum phase transitions in dimerized spin chains, *Phys. Rev. B* **82**, 052404 (2010).
- [15] C. Hang, G. Huang, and V. V. Konotop,  $\mathcal{PT}$  symmetry with a system of three-level atoms, *Phys. Rev. Lett.* **110**, 083604 (2013).
- [16] C. Korff and R. Weston, PT symmetry on the lattice: the quantum group invariant XXZ spin chain, *J. Phys. A* **40**, 8845 (2007).
- [17] C. Korff,  $PT$  symmetry of the non-Hermitian XX spin-chain: non-local bulk interaction from complex boundary fields, *J. Phys. A* **41**, 295206 (2008).
- [18] V. V. Konotop, J. Yang, and D. A. Zezyulin, Nonlinear waves in  $\mathcal{PT}$ -symmetric systems, *Rev. Mod. Phys.* **88**, 035002 (2016).
- [19] C. M. Bender and D. W. Hook,  $PT$ -symmetric quantum mechanics, [arXiv:2312.17386](https://arxiv.org/abs/2312.17386).
- [20] J. Cham, Top 10 physics discoveries of the last 10 years, *Nat. Phys.* **11**, 799 (2015).
- [21] L. Feng, R. El-Ganainy, and L. Ge, Non-Hermitian photonics based on parity-time symmetry, *Nat. Photon.* **11**, 752 (2017).
- [22] Y. Ashida, S. Furukawa, and M. Ueda, Parity-time-symmetric quantum critical phenomena, *Nat. Commun.* **8**, 15791 (2017).
- [23] K. Kawabata, Y. Ashida, and M. Ueda, Information retrieval and criticality in parity-time-symmetric systems, *Phys. Rev. Lett.* **119**, 190401 (2017).
- [24] S. Weimann, M. Kremer, Y. Plotnik, Y. Lumer, S. Nolte, K. G. Makris, M. Segev, M. Rechtsman, and A. Szameit, Topologically protected bound states in photonic parity-time-symmetric crystals, *Nat. Mater.* **16**, 433 (2017).
- [25] H. Menke and M. M. Hirschmann, Topological quantum wires with balanced gain and loss, *Phys. Rev. B* **95**, 174506 (2017).
- [26] K. Kawabata, Y. Ashida, H. Katsura, and M. Ueda, Parity-time-symmetric topological superconductor, *Phys. Rev. B* **98**, 085116 (2018).
- [27] J. A. S. Lourenço, R. L. Eneias, and R. G. Pereira, Kondo effect in a  $\mathcal{PT}$ -symmetric non-Hermitian Hamiltonian, *Phys. Rev. B* **98**, 085126 (2018).
- [28] H. Shen, B. Zhen, and L. Fu, Topological band theory for non-Hermitian Hamiltonians, *Phys. Rev. Lett.* **120**, 146402 (2018).
- [29] S. Yao, F. Song, and Z. Wang, Non-Hermitian Chern bands, *Phys. Rev. Lett.* **121**, 136802 (2018).
- [30] A. Fritzsche, T. Biesenthal, L. J. Maczewsky, K. Becker, M. Ehrhardt, M. Heinrich, R. Thomale, Y. N. Joglekar, and A. Szameit, Parity-time-symmetric photonic topological insulator, *Nat. Mater.* **23**, 377 (2024).
- [31] M. V. Berry, Quantal phase factors accompanying adiabatic changes, *Proc. R. Soc. A* **392**, 45 (1984).
- [32] Y. Aharonov and J. Anandan, Phase change during a cyclic quantum evolution, *Phys. Rev. Lett.* **58**, 1593 (1987).

- [33] D. J. Thouless, M. Kohmoto, M. P. Nightingale, and M. den Nijs, Quantized Hall conductance in a two-dimensional periodic potential, *Phys. Rev. Lett.* **49**, 405 (1982).
- [34] F. D. M. Haldane, Model for a quantum Hall effect without landau levels: Condensed-matter realization of the “parity anomaly,” *Phys. Rev. Lett.* **61**, 2015 (1988).
- [35] M. Z. Hasan and C. L. Kane, *Colloquium: Topological insulators*, *Rev. Mod. Phys.* **82**, 3045 (2010).
- [36] X.-L. Qi and S.-C. Zhang, Topological insulators and superconductors, *Rev. Mod. Phys.* **83**, 1057 (2011).
- [37] J. E. Moore, The birth of topological insulators, *Nature (London)* **464**, 194 (2010).
- [38] C. L. Kane and E. J. Mele, Quantum spin Hall effect in graphene, *Phys. Rev. Lett.* **95**, 226801 (2005).
- [39] C. L. Kane and E. J. Mele,  $Z_2$  topological order and the quantum spin Hall effect, *Phys. Rev. Lett.* **95**, 146802 (2005).
- [40] B. A. Bernevig and S.-C. Zhang, Quantum spin Hall effect, *Phys. Rev. Lett.* **96**, 106802 (2006).
- [41] J. E. Moore and L. Balents, Topological invariants of time-reversal-invariant band structures, *Phys. Rev. B* **75**, 121306(R) (2007).
- [42] L. Fu, C. L. Kane, and E. J. Mele, Topological insulators in three dimensions, *Phys. Rev. Lett.* **98**, 106803 (2007).
- [43] B. A. Bernevig and T. L. Hughes, *Topological Insulators and Topological Superconductors* (Princeton University Press, Princeton, NJ, 2013).
- [44] C. K. Chiu, J. C. Y. Teo, A. P. Schnyder, and S. Ryu, Classification of topological quantum matter with symmetries, *Rev. Mod. Phys.* **88**, 035005 (2016).
- [45] J. Gong and Q.-h. Wang, Time-dependent  $\mathcal{PT}$ -symmetric quantum mechanics, *J. Phys. A* **46**, 485302 (2013).
- [46] D.-J. Zhang, Q.-H. Wang, and J. Gong, Quantum geometric tensor in  $\mathcal{PT}$ -symmetric quantum mechanics, *Phys. Rev. A* **99**, 042104 (2019).
- [47] E. Sjöqvist, A. K. Pati, A. Ekert, J. S. Anandan, M. Ericsson, D. K. L. Oi, and V. Vedral, Geometric phases for mixed states in interferometry, *Phys. Rev. Lett.* **85**, 2845 (2000).
- [48] R. Bhandari, Singularities of the mixed state phase, *Phys. Rev. Lett.* **89**, 268901 (2002).
- [49] J. Anandan, E. Sjöqvist, A. K. Pati, A. Ekert, M. Ericsson, D. K. L. Oi, and V. Vedral, Anandan et al. reply, *Phys. Rev. Lett.* **89**, 268902 (2002).
- [50] P. B. Slater, Mixed state holonomies, *Lett. Math. Phys.* **60**, 123 (2002).
- [51] K. Singh, D. M. Tong, K. Basu, J. L. Chen, and J. F. Du, Geometric phases for nondegenerate and degenerate mixed states, *Phys. Rev. A* **67**, 032106 (2003).
- [52] D. M. Tong, E. Sjöqvist, S. Filipp, L. C. Kwek, and C. H. Oh, Kinematic approach to off-diagonal geometric phases of nondegenerate and degenerate mixed states, *Phys. Rev. A* **71**, 032106 (2005).
- [53] O. Andersson and H. Heydari, Operational geometric phase for mixed quantum states, *New J. Phys.* **15**, 053006 (2013).
- [54] C. E. Bardyn, L. Wawer, A. Altland, M. Fleischhauer, and S. Diehl, Probing the topology of density matrices, *Phys. Rev. X* **8**, 011035 (2018).
- [55] Z. C. Wang, Sub-geometric phases in density matrices, *Sci. Rep.* **9**, 13258 (2019).
- [56] M. Ericsson, E. Sjöqvist, J. Brännlund, D. K. L. Oi, and A. K. Pati, Generalization of the geometric phase to completely positive maps, *Phys. Rev. A* **67**, 020101(R) (2003).
- [57] A. Carollo, I. Fuentes-Guridi, M. F. Santos, and V. Vedral, Geometric phase in open systems, *Phys. Rev. Lett.* **90**, 160402 (2003).
- [58] J. G. P. d. Faria, A. F. R. d. T. Piza, and M. C. Nemes, Phases of quantum states in completely positive non-unitary evolution, *Europhys. Lett.* **62**, 782 (2003).
- [59] D. M. Tong, E. Sjöqvist, L. C. Kwek, and C. H. Oh, Kinematic approach to the mixed state geometric phase in nonunitary evolution, *Phys. Rev. Lett.* **93**, 080405 (2004).
- [60] L. C. Kwek, D. M. Tong, J. L. Chen, J. F. Du, K. W. Choo, R. Ravishankar, D. Kaszlikowski, and C. H. Oh, Geometric phase for mixed states, *Laser Phys.* **16**, 398 (2006).
- [61] O. Andersson, I. Bengtsson, M. Ericsson, and E. Sjöqvist, Geometric phases for mixed states of the Kitaev chain, *Philos. Trans. R. Soc. A* **374**, 20150231 (2016).
- [62] J. Du, P. Zou, M. Shi, L. C. Kwek, J.-W. Pan, C. H. Oh, A. Ekert, D. K. L. Oi, and M. Ericsson, Observation of geometric phases for mixed states using NMR interferometry, *Phys. Rev. Lett.* **91**, 100403 (2003).
- [63] A. Ghosh and A. Kumar, Experimental measurement of mixed state geometric phase by quantum interferometry using NMR, *Phys. Lett. A* **349**, 27 (2006).
- [64] J. Klepp, S. Sponar, S. Filipp, M. Lettner, G. Badurek, and Y. Hasegawa, Observation of nonadditive mixed-state phases with polarized neutrons, *Phys. Rev. Lett.* **101**, 150404 (2008).
- [65] M. Ericsson, D. Achilles, J. T. Barreiro, D. Branning, N. A. Peters, and P. G. Kwiat, Measurement of geometric phase for mixed states using single photon interferometry, *Phys. Rev. Lett.* **94**, 050401 (2005).
- [66] A. Uhlmann, Parallel transport and “quantum holonomy” along density operators, *Rep. Math. Phys.* **24**, 229 (1986).
- [67] A. Uhlmann, On berry phases along mixtures of states, *Ann. Phys.* **501**, 63 (1989).
- [68] A. Uhlmann, The metric of bures and the geometric phase, in *Groups and Related Topics: Proceedings of the First Max Born Symposium*, edited by R. Gielerek, J. Lukierski, and Z. Popowicz (Springer Netherlands, Dordrecht, 1992), pp. 267–274.
- [69] O. Viyuela, A. Rivas, and M. A. Martin-Delgado, Uhlmann phase as a topological measure for one-dimensional fermion systems, *Phys. Rev. Lett.* **112**, 130401 (2014).
- [70] O. Viyuela, A. Rivas, and M. A. Martin-Delgado, Two-dimensional density-matrix topological fermionic phases: Topological Uhlmann numbers, *Phys. Rev. Lett.* **113**, 076408 (2014).
- [71] H. Guo, X.-Y. Hou, Y. He, and C. C. Chien, Dynamic process and Uhlmann process: Incompatibility and dynamic phase of mixed quantum states, *Phys. Rev. B* **101**, 104310 (2020).
- [72] X.-Y. Hou, Q.-C. Gao, H. Guo, Y. He, T. Liu, and C. C. Chien, Ubiquity of zeros of the Loschmidt amplitude for mixed states in different physical processes and its implication, *Phys. Rev. B* **102**, 104305 (2020).
- [73] D. M. Galindo, F. Rojas, and J. A. Maytorena, Topological Uhlmann phase transitions for a spin- $j$  particle in a magnetic field, *Phys. Rev. A* **103**, 042221 (2021).

- [74] Y. Zhang, A. Pi, Y. He, and C.-C. Chien, Comparison of finite-temperature topological indicators based on Uhlmann connection, *Phys. Rev. B* **104**, 165417 (2021).
- [75] X.-Y. Hou, H. Guo, and C. C. Chien, Finite-temperature topological phase transitions of spin- $j$  systems in Uhlmann processes: General formalism and experimental protocols, *Phys. Rev. A* **104**, 023303 (2021).
- [76] X.-Y. Hou, X. Wang, Z. Zhou, H. Guo, and C.-C. Chien, Geometric phases of mixed quantum states: A comparative study of interferometric and Uhlmann phases, *Phys. Rev. B* **107**, 165415 (2023).
- [77] A. Das, Pseudo-Hermitian quantum mechanics, *J. Phys.: Conf. Ser.* **287**, 012002 (2011).
- [78] R. Zhang, H. Qin, and J. Xiao, PT-symmetry entails pseudo-Hermiticity regardless of diagonalizability, *J. Math. Phys.* **61**, 012101 (2020).
- [79] B. Gardas, S. Deffner, and A. Saxena, Non-Hermitian quantum thermodynamics, *Sci. Rep.* **6**, 23408 (2016).
- [80] Q. Du, K. Cao, and S.-P. Kou, Non-Hermitian Ising model at finite temperature, *Commun. Theor. Phys.* **75**, 045701 (2023).
- [81] J. Watrous, *The Theory of Quantum Information* (Cambridge University Press, Cambridge, 2018).
- [82] S. Lieu, Topological phases in the non-Hermitian Su-Schrieffer-Heeger model, *Phys. Rev. B* **97**, 045106 (2018).
- [83] S.-D. Liang and G.-Y. Huang, Topological invariance and global Berry phase in non-Hermitian systems, *Phys. Rev. A* **87**, 012118 (2013).
- [84] Q.-H. Wang, S. zhi Chia, and J. hong Zhang,  $\mathcal{PT}$  Symmetry as a generalization of Hermiticity, *J. Phys. A* **43**, 295301 (2010).
- [85] W. Heiss, The physics of exceptional points, *J. Phys. A* **45**, 444016 (2012).
- [86] M. S. Rudner and L. S. Levitov, Topological transition in a non-Hermitian quantum walk, *Phys. Rev. Lett.* **102**, 065703 (2009).
- [87] M. J. Rice and E. J. Mele, Elementary excitations of a linearly conjugated diatomic polymer, *Phys. Rev. Lett.* **49**, 1455 (1982).
- [88] J. K. Asbóth, L. Oroszlány, and A. Pályi, *A Short Course on Topological Insulators: Band-structure Topology and Edge States in One and Two Dimensions* (Springer, Berlin, 2016).
- [89] C. E. Rüter, K. G. Makris, R. El-Ganainy, D. N. Christodoulides, M. Segev, and D. Kip, Observation of parity-time symmetry in optics, *Nat. Phys.* **6**, 192 (2010).